JOURNAL OF VIROLOGY, Oct. 2000, p. 9601–9609 Vol. 74, No. 20
0022-538X/00/$04.00+0

Attenuation of Tick-Borne Encephalitis Virus by Structure-Based Site-Specific Mutagenesis of a Putative Flavivirus Receptor Binding Site

CHRISTIAN W. MANDL,* STEVEN L. ALLISON, HEIDEMARIE HOLZMANN, TAMARA MEIXNER, AND FRANZ X. HEINZ

Institute of Virology, University of Vienna, A-1095 Vienna, Austria

Received 6 April 2000/Accepted 10 July 2000

The impact of a specific region of the envelope protein E of tick-borne encephalitis (TBE) virus on the biology of this virus was investigated by a site-directed mutagenesis approach. The four amino acid residues that were analyzed in detail (E308 to E311) are located on the upper-lateral surface of domain III according to the X-ray structure of the TBE virus protein E and are part of an area that is considered to be a potential receptor binding determinant of flaviviruses. Mutants containing single amino acid substitutions, as well as combinations of mutations, were constructed and analyzed for their virulence in mice, growth properties in cultured cells, and genetic stability. The most significant attenuation in mice was achieved by mutagenesis of threonine 310. Combining this mutation with deletion mutations in the 3′-noncoding region yielded mutants that were highly attenuated. The biological effects of mutation Thr 310 to Lys, however, could be reversed to a large degree by a mutation at a neighboring position (Lys 311 to Glu) that arose spontaneously during infection of a mouse. Mutagenesis of the other positions provided evidence for the functional importance of residue 308 (Asp) and its charge interaction with residue 311 (Lys), whereas residue 309 could be altered or even deleted without any notable consequences. Deletion of residue 309 was accompanied by a spontaneous second-site mutation (Phe to Tyr) at position 332, which in the three-dimensional structure of protein E is spatially close to residue 309. The information obtained in this study is relevant for the development of specific attenuated flavivirus strains that may serve as future live vaccines.

Tick-borne encephalitis (TBE) *virus* is a human pathogenic member of the genus *Flavivirus* (family *Flaviviridae*) (31). Many members of this genus can cause severe human diseases, the most important representatives besides TBE virus being the mosquito-borne viruses yellow fever (YF) virus, Japanese encephalitis (JE) virus, and the four serotypes of dengue virus (18). In spite of the availability of attenuated live vaccines (in the case of YF virus) and formalin-inactivated killed vaccines (TBE virus, JE virus) which have proven to be effective for the prevention of flavivirus infections, there is a strong demand for the development of novel and improved vaccines against these and other flavivirus infections. For the rational design of live vaccines, a detailed understanding of the molecular basis of virulence and pathogenesis is a major goal. With the availability of modern molecular techniques and high-resolution structural information, it is now possible to alter viral structures in a specific and rational way in order to understand structure-function relationships. This knowledge can then be applied to achieve the desired biological property, such as attenuation of the virus.

Flavivirus virions are relatively simple particles consisting of a nucleocapsid composed of a single capsid protein (C) surrounded by a lipid membrane that contains two viral proteins, the small membrane protein M and the large envelope glycoprotein E (23). The nucleocapsid contains the viral genome, an unsegmented positive-stranded RNA of approximately 11 kb that is capped at the 5′ end but exhibits an elaborate RNA secondary structure rather than a poly(A) tail at its 3′ end (20). This RNA, which simultaneously serves as the only viral messenger, encodes all of the viral proteins (the three structural proteins C, M, and E and seven nonstructural proteins) in a single long open reading frame. The construction of infectious cDNA clones for a growing number of flaviviruses, including TBE virus (24), during the past 10 years has made it possible to specifically mutate flaviviruses and study the effects of individual mutations on the biology of these viruses. For instance, certain deletions engineered into the 3′-noncoding region (NCR) of TBE virus have been shown to produce strong attenuation of this virus in the mouse model (16).

The envelope protein E appears to be particularly important for virulence, since it is responsible for some of the most crucial functions during the flavivirus life cycle: it mediates primary attachment of the virus to its target cell and thus determines, at least in part, the host-cell tropism and pathogenesis of the virus. After attachment and uptake of the virus by endocytosis, protein E is triggered by an acid-induced conformational change to mediate fusion of the viral and cellular membranes enabling the nucleocapsid to be released into the cytoplasm. Protein E is also the major target of neutralizing antibodies produced by the host and by itself is sufficient to elicit a protective immune response. The solution of the atomic structure of the ectodomain of protein E of TBE virus by X-ray crystallography (22) revealed that this protein does not form protruding spikes that are perpendicular to the viral surface but instead is arranged as a head-to-tail homodimer that is oriented parallel to the viral membrane. Each monomer consists of three structurally distinct domains, referred to as domain I (central domain), domain II (dimerization domain), and domain III, which exhibits the characteristic fold of an immunoglobulin constant domain.

Analysis of mutants of different flaviviruses with altered vir-

* Corresponding author. Mailing address: Institute of Virology, University of Vienna, Kinderspitalgasse 15, A-1095 Vienna, Austria. Phone: 43-1-404-90, ext. 79502. Fax: 43-1-406-21-61. E-mail: christian.mandl@univie.ac.at.

TABLE 1. Primers used for mutagenesis

Orientation	Sequence[a]	Amino acid mutation(s)
Sense	5′-TCT*TACGTA*CACAATGTGTAAGAAAACAAAGTT-3′	308Asp→Lys
Sense	5′-TCT*TACGTA*CACAATGTGTGACTTAACAAAGTT-3′	309Lys→Leu
Sense	5′-TCT*TACGTA*CACAATGTGTGACA-Δ-CAAAGTTCACATGG-3′	Δ309
Sense	5′-TCT*TACGTA*CACAATGTGTGACAAAAAAAAGTTCAC-3′	310Thr→Lys
Sense	5′-TCT*TACGTA*CACAATGTGTGACAAAACAGAGTTCACAT-3′	311Lys→Glu
Sense	5′-TCT*TACGTA*CACAATGTGTAAGAAAACAGAGTTCACAT-3′	308Asp→Lys and 311Lys→Glu
Sense	5′-TCT*TACGTA*CACAATGTGTGACAAAAAAGAGTTCACAT-3′	310Thr→Lys and 311Lys→Glu
Antisense	5′-CTGACTG*GGATCC*TACAGGG-3′	

[a] Restriction enzyme recognition sequences are shown in italics; nucleotide substitutions are underlined; "Δ" indicates a three-nucleotide deletion.

ulence properties including tissue-culture-adapted mutants, neutralization escape mutants, naturally occurring virus variants, vaccine strains and, most recently, mutants generated by site-specific mutagenesis (reviewed in reference 17) has revealed numerous mutations within protein E that influence virulence and pathogenesis. Interestingly, mapping of these mutations on the molecular structure of protein E indicated that they formed three distinct clusters (22). First, there are mutations at or near the tip of domain II, which is believed to contain the fusion peptide. Another cluster is located within a predicted hinge region connecting domains I and II, which is probably involved in the acid-induced conformational change. Thus, the mutations of these two clusters are likely to affect virulence by influencing fusion activity. The third cluster is on the upper and distal-lateral surface of domain III, which has been proposed to be involved in receptor binding, and this may be the functional basis of how these mutations influence the virulence of flaviviruses. Aside from dengue type 2 virus, for which a requirement for heparan sulfate binding has been demonstrated (2), no specific flavivirus cellular receptors have been definitively identified, but some reports indicate the presence of various cell surface proteins with specific binding affinities for different flaviviruses (10, 11, 19, 27). An involvement of the lateral surface of domain III in cell attachment is suggested by several lines of indirect evidence (12, 22), including the immunoglobulin-like fold of this domain, which is characteristically found in many proteins with specific binding functions, the high density of charged surface residues on the lateral surface, the presence of an RGD motif in some mosquito-borne flaviviruses (which is known in other cases to be recognized by members of the integrin protein familiy), and the identification of mutations in this region in host range mutants (14) and mutants with altered virulence properties (1, 3, 4, 8, 9, 13, 26).

In this study we introduced mutations at four positions (residues 308 to 311) of the upper-lateral surface of domain III of the TBE virus protein E and investigated their influence on biological properties of the resulting mutant viruses. For each position distinct effects on the genetic stability, growth properties in cell culture, and virulence in mice were observed. Most importantly, a substitution of position 310 from Thr to Lys resulted in significant attenuation, which could be further enhanced by combining this mutation with previously described deletion mutations in the 3′-NCR.

MATERIALS AND METHODS

Virus and infectious cDNA clone. All mutants were derived from prototype strain Neudoerfl of Western subtype TBE virus, which was also used as the wild-type control in all experiments. The biological properties of this virus, including virulence, have been previously characterized in detail (16), and its complete genomic sequence is known (GenBank accession no. U27495). Specific mutants of this virus strain were engineered using previously described cDNA clones from which infectious RNA was transcribed in vitro (15). Plasmid pTNd/c contains cDNA corresponding to the entire genome of TBE virus strain Neudoerfl. Plasmids pTNd/5′ and pTNd/3′ contain cDNAs corresponding to the 5′ one-third and the 3′ two-thirds of the genome, respectively, and after in vitro ligation infectious full-length RNA can be transcribed from these plasmids. Plasmids pTNd/3′Δ10847 and pTNd/3′Δ10919 contain deletions within the 3′-NCR extending from the stop codon of the single long open reading frame to the designated position. These plasmids and the properties of the virus mutants derived from them were described previously (16).

Cloning procedures. All protein E mutations were introduced into plasmid pTNd/5′ by swapping the small (110 bp) *Sna*BI (at position 1878 of the TBE strain Neudoerfl genome)-*Bam*HI (at position 1988) fragment with a PCR-derived fragment containing the desired mutation(s). Both *Sna*BI and *Bam*HI have unique recognition sequences within pTNd/5′. The sequences of the mutagenic sense primers and the antisense primer which were used for all constructs are listed in Table 1.

Virus recovery and stock virus preparations. The mutated derivatives of plasmid pTNd/5′ and plasmid pTNd/3′ or its derivatives carrying 3′-NCR deletion mutations (16) were joined by in vitro ligation at the unique *Cla*I restriction site to give full-length templates for subsequent RNA transcription by T7 RNA polymerase. The generation of genome-length RNA, its purification, and its transfection into BHK 21 cells by electroporation were performed as described elsewhere (15). Three to five days after electroporation, cell culture supernatants were usually found to be positive for TBE virus protein E using a four-layer enzyme-linked immunosorbent assay (ELISA) (6). In order to achieve sufficient amounts of high-titer virus stocks with a minimum of viral passages, litters of suckling mice were infected intracranially with the cell culture supernatant. Virus was then passaged a second time in suckling-mouse brain, and 20% (wt/vol) suspensions of brain homogenate were prepared to serve as virus stocks for all subsequent experiments.

Sequence analysis. Sequencing was performed with an automated DNA sequencing system (ABI–Perkin-Elmer). New plasmid constructions were checked by sequence analysis over the entire protein E coding region and in the vicinity of restriction sites used for cloning. The protein E coding region of all mutant virus stocks and from virus present in the brain of two adult mice killed by each mutant was sequenced. For these analyses, genomic RNA was purified from suckling mouse or adult mouse brains and analyzed by reverse transcription-PCR (RT-PCR) by standard methods and as described previously (29). PCR-derived fragments were sequenced directly and on both strands.

Cell cultures. BHK-21 cells, porcine kidney (PS) cells, and primary chicken embryo (CE) cells were grown under standard conditions as described previously (7, 15). Infectivity values of virus stocks were determined by plaque titer determinations on PS cells (7) and confirmed by endpoint dilution infection experiments on BHK-21 and CE cells. To test for temperature sensitivity, plaque tests were performed at the standard incubation temperature (37°C) and at an elevated temperature (40°C), and the number and morphology of the plaques were evaluated. Growth capacities in CE cells were determined as described in detail elsewhere (15). Briefly, cells were infected at a multiplicity of infection (MOI) of approximately 1, and virus released from the cells within 1-h periods was collected from the supernatant at several times postinfection. The infectious titers of these samples were determined by standard plaque assays.

Animal model. Virulence and infectivity characteristics were analyzed in outbred Swiss albino mice. Groups of 10 5-week-old (body weight, approximately 20 g) mice were inoculated subcutaneously, and survival was recorded for 28 days. Mice were then bled, and seroconversion was investigated by a TBE virus-antibody ELISA (5). For the determination of the 50% lethal dose (LD_{50}) and the 50% infectious dose (ID_{50}), mice were inoculated with sequential 10-fold dilutions of virus ranging from 1 to 10^5 (and 10^6, where appropriate) PFU. The calculation of LD_{50} and ID_{50} values was performed by the method of Reed and Muench (21). For ID_{50} calculations, the number of infected mice was taken to be the total of mice killed plus the surviving mice with detectable seroconversion. Surviving mice without detectable serum antibody were scored as uninfected. To test whether seroconverted mice had developed a protective immunity, mice were inoculated with a challenge dose of 100 LD_{50} of the highly virulent TBE virus strain Hypr (30).

Protein structure graphics. The three-dimensional structure of a soluble ectodomain fragment of the TBE virus envelope protein at 2.0 Å resolution (22) (PDB entry 1SVB) was used as the basis for all depictions of protein E and models of mutants. The software program Insight II, version 95.0 (Biosym/MSI, San Diego, Calif), was used for protein structure graphics and the Homology module of this program was used for modeling loops and side chain rotamers.

RESULTS

Mutagenesis of the upper-lateral surface of protein E. The amino acid residues 308, 309, 310, and 311 of the TBE virus protein E were selected for our study. These four amino acids form an extended loop of the upper-lateral surface of protein E. The topography of this site on the protein E dimer and a detailed view of our region of interest are shown in Fig. 1. A striking structural feature of this area is its high content of charged amino acid side chains. In particular, the negatively charged residue 308 (Asp) and the positively charged residue 311 (Lys) are in close proximity, enabling the formation of a salt bridge between these two residues (22). The polar, but uncharged side chain of residue 310 (Thr) protrudes below this salt bridge, whereas the side chain of Lys 309 is located on the other side of Asp 308, but is too far away to intimately interact with its neighbor. Comparison of various flavivirus sequences reveals that Lys 309 is conserved among all tick-borne flaviviruses, but this residue is absent from the mosquito-borne flavivirus sequences (22).

We constructed TBE virus mutants that carried single point mutations at each of the four positions 308 to 311, mutants that carried combinations of two of these mutations, and mutants with a single protein E mutation coupled with a specific deletion in the 3′-NCR (16). All mutants generated in this study are listed in Table 2 and were analyzed according to exactly the same experimental scheme. For clarity, results are summarized for each mutant or set of related mutants and presented in separate sections below.

Amino acid Lys 309. Two different mutations were introduced at this position. First, since Lys 309 is present in all tick-borne flavivirus sequences but absent from the mosquito-borne flaviviruses, this residue was deleted. In a second construct, Lys 309 was replaced by a Leu residue, a nonpolar uncharged residue of similar size. We anticipated that this mutation would be more likely to yield viable virus than the deletion mutation but would still be useful for clarifying the functional importance of the positive charge at position 309. Indeed, the corresponding mutant virus, designated E(K309L), was readily obtained from transfected BHK-21 cells, whereas in the case of the clone carrying the deletion mutation, we recovered virus in only one of three independently performed experiments. Nevertheless, sufficiently high-titer virus stocks of both mutant viruses could be prepared from infected suckling baby mouse brains (Table 2), and these were subjected to sequence analysis of the genomic protein E coding region. This confirmed the presence of the engineered mutations for both mutants, but in the case of the position 309 deletion mutant an additional mutation (Phe 332 to Tyr) was found [E(Δ309/F332Y); Table 2]. Inspection of the atomic structure suggests a causal link between the engineered deletion and the emergence of the secondary mutation. As shown in Fig. 2, residue 332 is located immediately behind residue 309. The additional hydroxyl group gained by the Phe-to-Tyr substitution may help to fill the gap created by the deletion and thus be able to structurally compensate for this mutation. It is likely that the deletion caused a displacement of the main chain, because in the wild-type structure a Tyr at position 332 would collide with the main chain amino group of residue 308 (Fig. 2).

To our surprise, the biological characterization of the two amino acid 309 mutants did not reveal any significant differences compared to the wild-type strain Neudoerfl. They both exhibited normal plaque morphologies on PS cells, and plaque assays performed at an elevated temperature (40°C) did not provide any evidence for temperature sensitivity with respect to infectivity titers or plaque morphologies (Table 2). Similarly, quantitative growth curves determined on CE cells infected at an MOI of 1 revealed no differences in the cell culture growth capacities of these mutants compared to the wild-type virus. Figure 3 compares the amount of infectious virus released at two selected time points, one during the early phase of infection (12 h postinfection [p.i.]) and the other one within the plateau phase of virus release (21 h p.i.). In the adult mouse model (Fig. 4), both mutants proved to be almost as virulent (as measured by the LD_{50}) and infectious (as determined by the ID_{50}) as the wild-type control virus. In order to check for genetic stability during infection of the adult mouse, viral RNA from the brains of two mice killed by each mutant was sequenced over the protein E coding region. No sequence reversions or additional mutations were detected in these cases.

Amino acids Asp 308 and Lys 311. These two charged residues form a salt bridge and this interaction may be important for the structural integrity and functionality of this protein domain. To test this hypothesis, we designed mutations that would reverse the charge polarity of one of the partners of the salt bridge (Asp 308 to Lys, and Lys 311 to Glu, respectively) and therefore eliminate this structure. In addition, we constructed a double mutant containing both of these mutations, which would potentially allow the formation of a salt bridge in the inverted orientation. Infectious virus was readily obtained from all three constructs, and virus stocks with high infectivity titers were prepared (Table 2). In the cases of mutant viruses E(K311E) and E(D308K/K311E), sequencing confirmed the desired mutations and revealed no additional mutations in the E gene. In the case of the single point mutation at amino acid 308, however, the Lys substitution was unstable and spontaneously changed to a Glu after two passages in baby mouse brain (Table 2). The desired Lys mutation was still present after the first baby mouse passage, but a second passage of this virus in either baby mice or adult mice again selected for a Glu residue at position 308 (data not shown). A back-mutation from Lys to the original Asp sequence would have required two separate nucleotide changes, whereas only a single base change was necessary to produce a codon for Glu which, like Asp, has a negative charge. In accordance with the mutation that was actually present, this mutant was designated E(D308E).

The biological characterizations of mutants E(D308E) and E(K311E) revealed wild-type plaque morphologies and no temperature sensitivity (Table 2). The growth behavior of these two mutants on CE cells was also indistinguishable from the wild-type virus (Fig. 3). The double mutant E(D308K/K311E), however, exhibited altered plaque morphologies at both incubation temperatures (Table 2). Moreover, there was an approximately 10-fold reduction in the amount of infectious virus in the supernatant of CE cells during the plateau phase of infection with this mutant (Fig. 3).

The double mutant also exhibited the most distinguishing phenotype in the adult mouse model (Fig. 4). It was found to be >1,000-fold less virulent than the wild type (its LD_{50} was 10^4 PFU compared to <10 PFU for wild-type virus). However, its overall infectivity (ID_{50}) upon peripheral subcutaneous inoculation was also somewhat reduced compared to the wild type. We used the LD_{50}/ID_{50} ratio, which we refer to as the attenuation index, to correct for differences in the ID_{50} in order to reveal the degree to which neuroinvasiveness itself, rather than the overall infectivity, was reduced. We found that

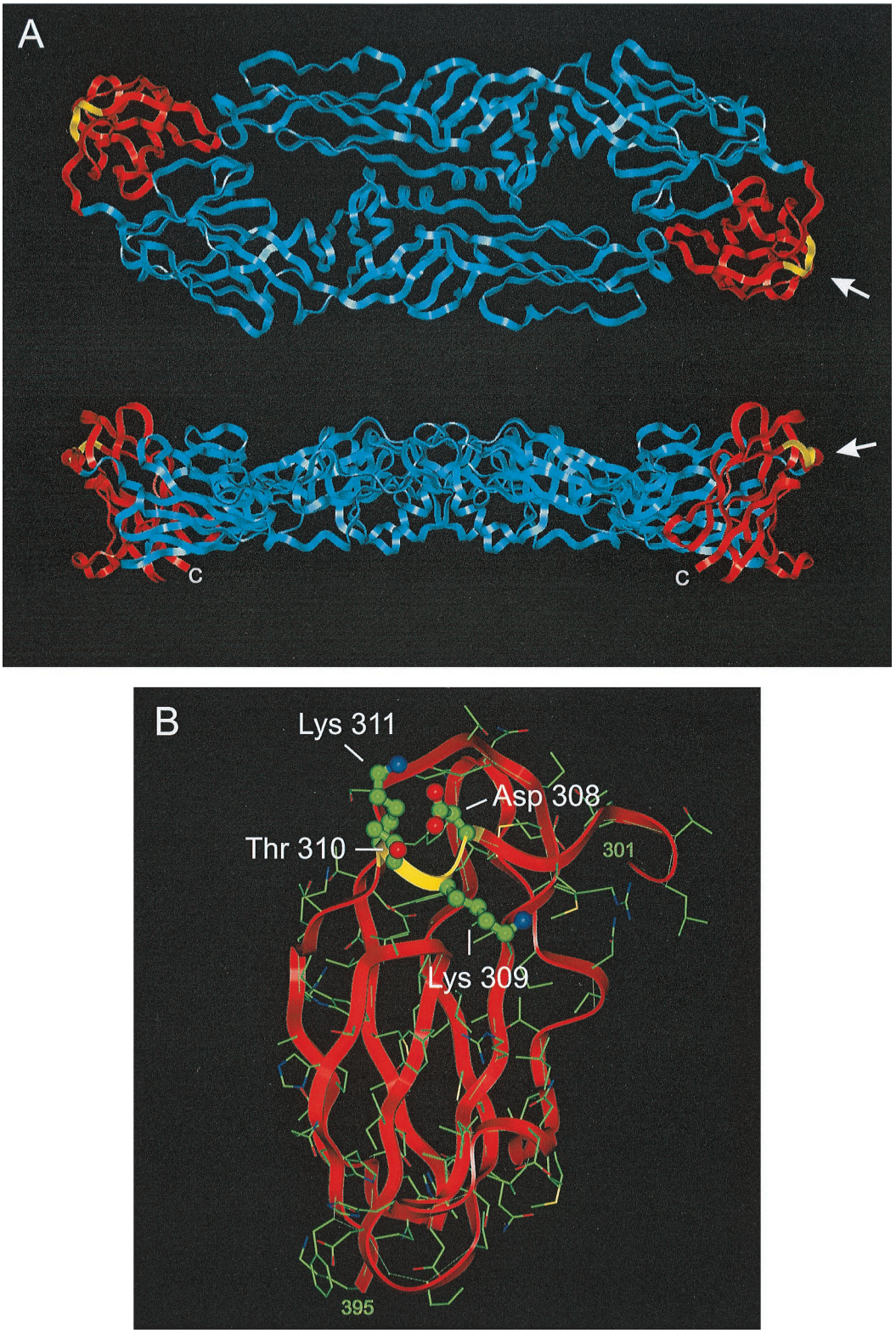

FIG. 1. Topography of Asp 308, Lys 309, Thr 310, and Lys 311 on the TBE virus E protein. (A) Top view (upper) and side view (lower) of the ectodomain region of the E dimer (22) with the main chain shown as a ribbon. Blue, domains I and II; red, domain III; yellow, residues 308 to 311. The carboxy terminus of each subunit, which in the full-length E protein is contiguous with the stem-anchor region, is indicated by a "C". (B) Enlarged image of domain III as viewed from the direction of the arrows in panel A. The α carbons and side chains of each residue are shown with the hydrogen atoms omitted. Amino acids 308 to 311 are shown as ball-and-stick forms; the others are shown as lines. Atom colors: green, carbon; blue, nitrogen; red, oxygen; yellow, sulfur. The N and C termini of domain III (residues 301 and 395, respectively) are indicated.

TABLE 2. TBE virus mutants

Mutant virus	Engineered mutation(s)[a]		Spontaneous mutation(s)[d]		Infectivity titer of stock solution (PFU/ml)	Plaque morphology[f] at:	
	Nucleotide[b]	Amino acid[c]	Nucleotide[b]	Amino acid[c]		37°C	40°C
E(Δ309/F332Y)	Δ1897–1899	Δ309 Lys	1967 T→A	332 Phe→Tyr	3×10^8	WT	WT
E(K309L)	1897 A→T 1898 A→T	309 Lys→Leu	None		1×10^8	WT	WT
E(D308E)	1894 G→A 1896 C→G	308 Asp→Lys	1894 A→G	308 Lys→Glu	5×10^8	WT	WT
E(K311E)	1903 A→G	311 Lys→Glu	None		4×10^8	WT	WT
E(D308K/K311E)	1894 G→A 1896 C→G 1903 A→G	308 Asp→Lys 311 Lys→Glu	None		3×10^8	(S, T)[g]	S, T
E(T310K)	1901 C→A	310 Thr→Lys	1859 A→G 1903 A→G	296 Lys→Arg 311 Lys→Glu	5×10^9	S	S, T
E(T310K/K311E)	1901 C→A 1903 A→G	310 Thr→Lys 311 Lys→Glu	None		5×10^8	WT	WT
E(T310K)3′(Δ10847)	1901 C→A Δ10378–10847[e]	310 Thr→Lys	None		4×10^7	S	S, T
E(T310K)3′(Δ10919)	1901 C→A Δ10378–10919[e]	310 Thr→Lys	None		2×10^8	S, T	S, T

[a] E protein mutations engineered into plasmid pTNd/5′ (15); 3′-NCR deletion mutations engineered into plasmid pTNd/3′ were as described previously (16). Δ, Deletion.
[b] Numbers are according to TBE virus genomic sequence GenBank accession no. U27495.
[c] Numbers starting from the amino terminus of protein E.
[d] Mutations emerged during baby mouse brain passages [in the cases of mutants E(Δ309/F332Y) and E(D308E)] or infection of an adult mouse [in the case of E(T310K)].
[e] Deletions in the 3′-NCR as described previously (16).
[f] WT, wild-type morphology (clear plaques, diameter of 2 to 4 mm); S, small plaques (diameter of <2 mm); T, turbid plaques.
[g] Heterogeneous morphology with some clear and large plaques.

the attenuation index for the double mutant was about 100-fold higher than that of the wild-type virus.

Unexpectedly, mutant E(D308E), although differing from the wild-type by only a conservative mutation, exhibited a distinct phenotype in the mouse model. Both the LD_{50} and the ID_{50} were found to be elevated to a similar degree, and therefore the attenuation index was not significantly changed. Thus, the main effect of this mutation apparently was a reduction of peripheral infectivity rather than neuroinvasiveness itself. In contrast, mutation of residue E311 had little effect on the virulence and infectivity of TBE virus, as demonstrated by mutant E(K311E), which exhibited normal LD_{50} and ID_{50} values. Genetic alterations during infection of the adult mouse were not observed for these three mutants.

Amino acid Thr 310. Amino acid Thr 310 is a polar but uncharged residue embedded in an environment that carries a high density of charged amino acids. Changing this residue into a Lys would add an additional positive charge to this region

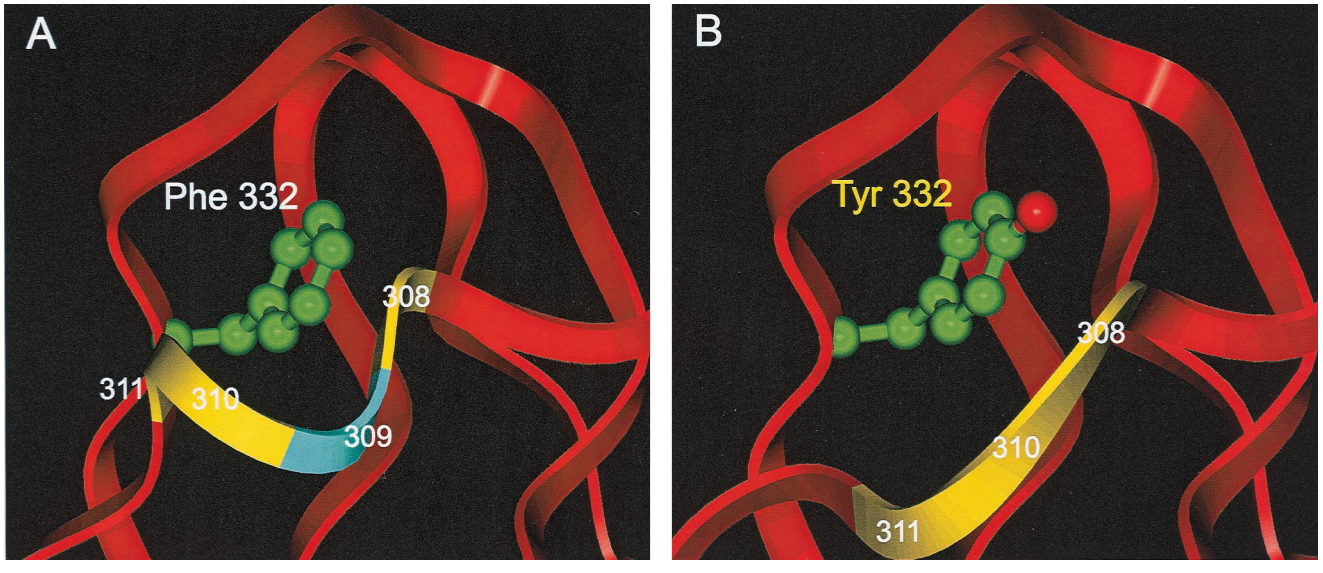

FIG. 2. Spatial relationship between residues 308 to 311 and residue 332. The view is a zoom of the annotated portion of Fig. 1B. (A) Wild-type, showing Phe 332 as a ball-and-stick representation. The portion of the ribbon corresponding to Lys 309 is colored light blue. (B) Model representing mutant E(Δ309/F332Y), with Lys 309 deleted and a compensating Phe-to-Tyr mutation at position 332.

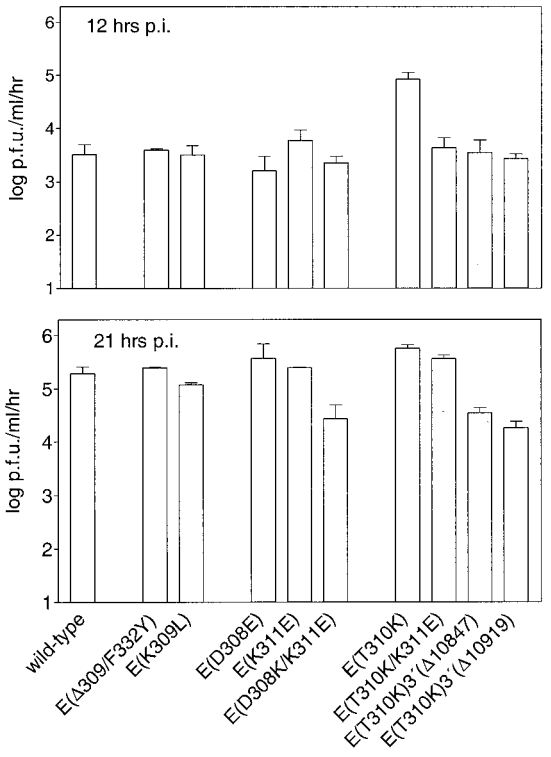

FIG. 3. Growth capacities of wild-type (strain Neudoerfl) and mutant TBE viruses on primary CE cells infected with an MOI of 1. The values plotted were derived from duplicate experiments. The amount of infectious virus released into the cell culture supernatant during a 1-h time period was determined 12 h p.i. (upper panel) and 21 h p.i. (lower panel).

and thus have a major effect on its surface properties. This was found to have profound consequences on the biological properties of the virus, and it showed an altered phenotype in almost all of the parameters tested in this study.

The infectivity titer achieved for the virus stock of mutant E(T310K) was higher (5×10^9 PFU/ml) than for all of the other viruses, including the wild-type parent strain. It exhibited a small, clear plaque phenotype at 37°C and small, turbid plaques at the elevated temperature (Table 2). On CE cells (Fig. 3), significantly more infectious particles of this mutant were released into the supernatant during the early time period (12 h p.i.) than for any of the other mutants or wild-type virus. The maximum value of virus release as measured in the plateau phase (21 h p.i.) was only slightly higher than that of the wild type.

In the adult mouse model (Fig. 4), E(T310K) was found to be strongly attenuated: the LD_{50} was more than 10,000-fold higher than the wild-type level. Although the infectivity of this mutant was also impaired by a factor of approximately 100, it still achieved a higher attenuation index than mutant E(D308K/K311E).

The protein E coding sequences of virus isolated from the brains of two mice killed by the infection were checked to assess the genetic stability of the mutations during the journey of the virus from the peripheral inoculation site to the brain. In the case of E(T310K), virus isolated from one of the two mice exhibited two novel mutations (Table 2). (i) Nucleotide 1859 was changed from A to G, causing a conservative amino acid change at position E296 from Lys to Arg. (ii) Nucleotide 1903 was changed from A to G, causing a change of amino acid E311 from Lys to Glu. Significantly, this second mutation is at a position adjacent to the engineered mutation at position 310 (Thr to Lys).

Amino acid 310 (Thr to Lys) in combination with amino acid 311 (Lys to Glu). To test whether the above described mutation at position 311, which had emerged during infection of one of the adult mice with mutant E(T310K), was responsible for the phenotypic reversion of this mutant, the corresponding mutations (Thr 310 to Lys and Lys 311 to Glu) were engineered into the infectious cDNA clone and mutant E(T310K/K311E) was generated. Sequence analysis of the stock virus from baby mouse brain demonstrated that this combination of mutations is genetically stable.

The biological analysis of E(T310K/K311E) indicated that the biological effects caused by the E310 Thr-to-Lys mutation were at least in part reversed by the second mutation at the neighboring location. With respect to the infectivity titer of the virus stock, its plaque morphology (Table 2), and its cell culture growth properties (Fig. 3), mutant E(T310K/K311E) was indistinguishable from the wild type, whereas mutant E(T310K) had been shown to be different in all of these parameters. With respect to virulence in the adult mouse model (Fig. 4) mutant E(T310K/K311E) exhibited LD_{50} and ID_{50} values that were between those observed for wild-type virus and mutant E(T310K) but had an almost wild-type level attenuation index. Thus, we conclude that mutant E(T310K/K311E)

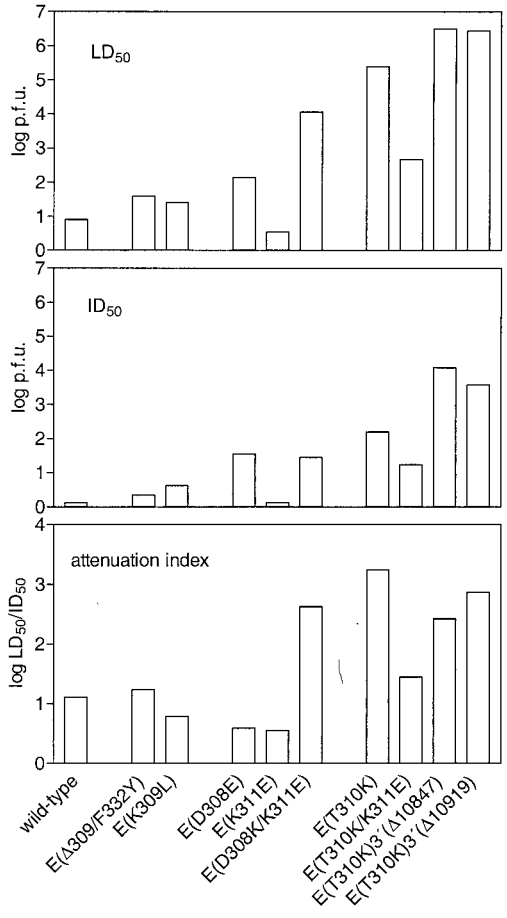

FIG. 4. Virulence and infectivity of wild-type (strain Neudoerfl) and mutant TBE viruses tested by subcutaneous inoculation of 5-week-old mice. LD_{50} (top panel) and ID_{50} (middle panel) values were determined as described in Materials and Methods. The attenuation index (bottom panel) was calculated as the LD_{50}/ID_{50} ratio.

more closely resembled the virulent wild-type virus rather than the single-amino-acid mutant E(T310K), with the exception that it exhibited an impaired peripheral infectivity compared to wild-type virus.

Amino acid 310 (Thr to Lys) in combination with deletions in the 3′-NCR. Of the protein E mutants analyzed, the most significant attenuation had been obtained by the mutation of 310 Thr to Lys. Previously, we observed that certain deletions in the 3′-NCRs of TBE virus also caused significant attenuation while maintaining good peripheral infectivity (16). To test whether these two attenuating principles could be combined in an additive or even cooperative manner, we designed two mutants that contained both the Thr 310-to-Lys mutation and one of two different 3′-NCR deletions that had been studied previously (Table 2). Sequence analysis of the protein E coding regions and the 3′-NCRs of the derived viral mutants confirmed the presence of the desired changes, but no additional mutations were detected. The infectivity titer of the E(T310K) 3′(Δ10847) mutant was somewhat lower than for the other mutants. Both mutants exhibited a small-plaque phenotype and turbid plaques at the elevated temperature, similar to mutant E(T310K), which contains the same protein E mutation but a wild-type 3′-NCR. For mutant E(T310K)3′(Δ10919) plaques were turbid already at the standard incubation temperature (Table 2). In contrast to E(T310K), both mutants released only wild-type levels of infectious virus into the supernatant of infected CE cells at 12 h p.i. and significantly lower levels at 21 h p.i. (Fig. 3).

In the adult mouse model (Fig. 4), both mutants that combined mutation Thr 310 to Lys with 3′-NCR deletions were found to be almost completely apathogenic. In the case of mutant E(T310K)3′(Δ10847), not a single mouse was killed at any inoculation dose. In the case of mutant E(T310K) 3′(Δ10919), one mouse was killed at the highest inoculation dose (10^6 PFU). However, the combination of these two attenuating principles also strongly impaired the peripheral infectivity of these two mutants, as demonstrated by the elevated ID_{50} values. Due to the inability to achieve even higher inoculation doses, it was not possible to calculate true LD_{50} values for these two mutants. The LD_{50} and the derived LD_{50}/ID_{50} attenuation index values shown in the figure thus represent the lowest possible estimates calculated under the assumption that an inoculation dose of 10^7 PFU would have killed all of the mice. It seems fair to assume, however, that the real values would turn out to be significantly higher than those shown in the figure.

Both of these highly attenuated combination mutants induced a solid protective immunity. We observed that every animal that had seroconverted (and this was the parameter on which the ID_{50} calculations were based) was completely protected against a subsequent challenge with a 100-fold lethal dose of virulent TBE virus (data not shown).

DISCUSSION

There is considerable evidence that the upper lateral surface of the flavivirus protein E is part of an important functional determinant. Indirect evidence for this assumption has been derived from the molecular structure of the TBE virus protein E, as well as from studies on various flavivirus mutants. Recognition of a still-unidentified flavivirus cell surface receptor is the most likely function associated with this region. Some mosquito-borne flaviviruses contain an RGD sequence motif at a position corresponding to a four-amino-acid insert between amino acids 386 and 387 in the TBE sequence (22). RGD motifs are known to mediate the binding of cellular or viral proteins to members of the integrin protein family (25). However, a recent mutagenesis study of YF virus strain 17D demonstrated that integrins do not function as major receptors for this virus (28). The four-amino-acid insert of mosquito-borne flaviviruses probably forms a loop that may cover or at least interact with the upper lateral surface region that was investigated for TBE virus in this study. This region is also part of one of the two potential heparan sulfate binding sites that have been described for dengue type 2 virus (2). The data presented in this study demonstrate, however, that none of the four investigated amino acid residues are absolutely essential for the specific recognition of a receptor, because substitutions at each of the four positions yielded viable virus. The lack of a rigid requirement for particular amino acid interactions suggests that this region is not the only determinant of virus attachment.

For the purpose of this discussion, we have constructed simplified models of the upper-lateral surface (Fig. 5). In reality, the mutations would probably also induce conformation alterations of the main chain, making the pictures more complex. The results obtained by our approach suggest a prominent functional role of residue Thr 310. Changing this residue into a positively charged and much bulkier Lys residue (Fig. 5C) had clear effects on the biology of TBE virus: the virus grew faster and to high titers in tissue culture and in baby mouse brain but exhibited a small-plaque phenotype. Its neuroinvasiveness after the peripheral inoculation of adult mice was significantly reduced. These observations are compatible with the idea that changing residue 310 to Lys affects the affinity of virus for certain cell surfaces in a way that accelerates virus production but simultaneously impedes virus spread from cell to cell. A mutation of position 310 from Ser to Pro had previously been identified in a neutralization escape mutant of Louping ill (LI) virus, a closely related tick-borne flavivirus. This mutant was reported to show partially reduced virulence but exhibited a wild-type plaque morphology (9). We show here that the effects of the mutation of Thr 310 to Lys could, to a large extent, be reversed by a secondary mutation of Lys 311 to Glu, indicating that there is not an absolute requirement for Thr per se in this position. This mutation was also observed to arise spontaneously during infection of an adult mouse. It is possible that this second mutation simply neutralized the additional positive charge introduced by the first mutation. Alternatively, as shown in Fig. 5D, this second mutation might serve to bring Lys 310 into a different position through its charge attraction and thus possibly alleviate steric hindrance of receptor binding caused by the bulky Lys residue. Interestingly, a mutation of YF virus Lys 303 to Gln (which by sequence alignment is shown to be equivalent to TBE residue 311) was found to be responsible for a strongly increased virulence in a mutant strain isolated from a vaccine-associated fatal human infection (8).

The X-ray crystal structure of protein E shows that residues Asp 308 and Lys 311 interact to form a salt bridge (Fig. 5A). Our observation that the Asp 308-to-Lys mutation spontaneously reverted to a negatively charged Glu residue demonstrates the structural importance of this interaction. This view is further corroborated by the fact that changing Asp 308 to Lys in combination with Lys 311 to Glu yielded a genetically stable mutant without a tendency for back-mutation at position 308. As shown in Fig. 5B, this double mutant can be imagined to form a salt bridge in a reversed orientation compared to the wild type. On the other hand, changing the charge on the other side of the salt bridge mutating Lys 311 to Glu yielded a genetically stable, virulent, and highly infectious virus. Clearly, this mutation also eliminates the 308–311 salt bridge, but this

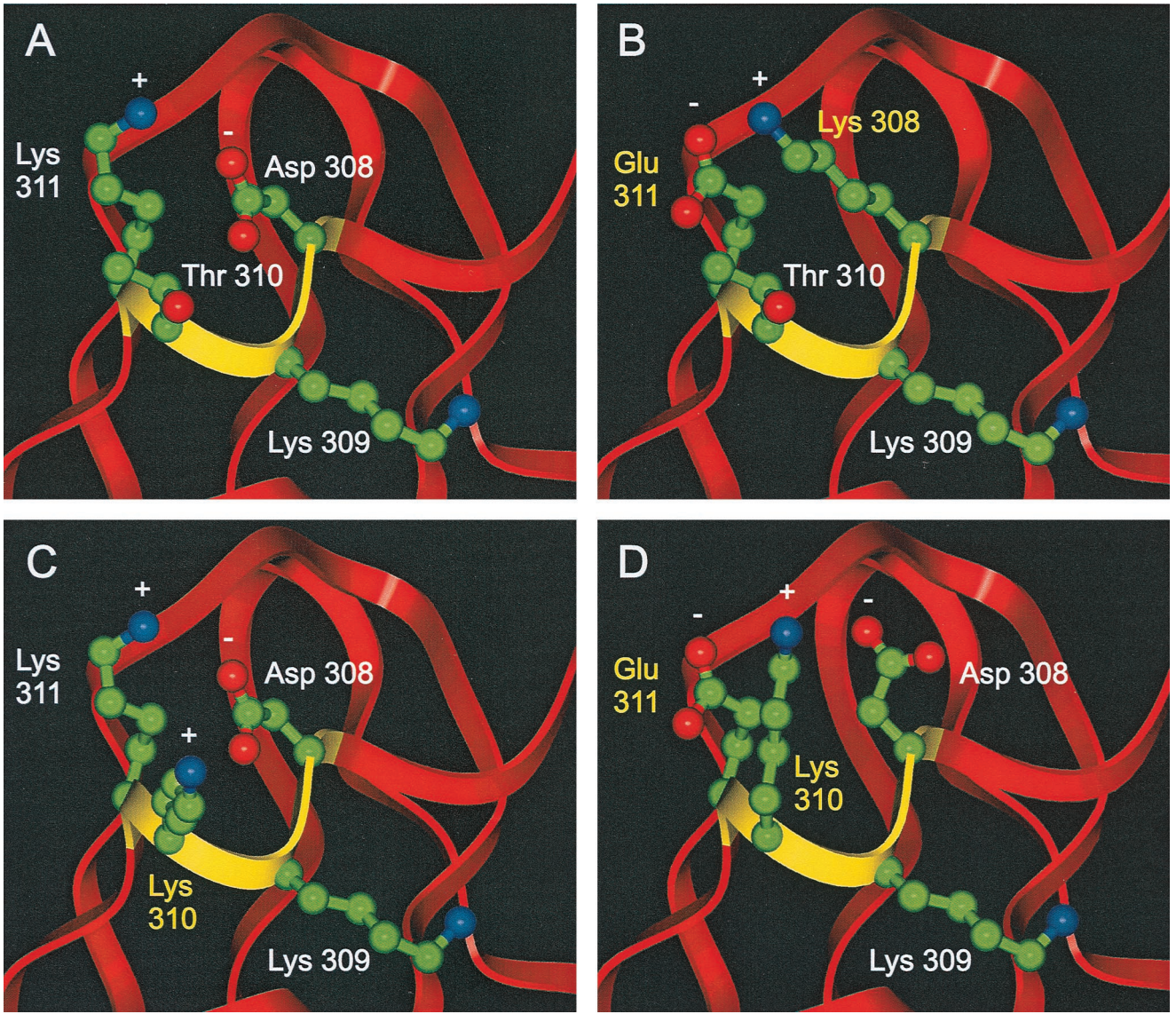

FIG. 5. Proposed interactions of charged side chains in mutants of TBE virus. The view is a zoom of Fig 1B (see Fig. 1 legend for details). Charge interactions between the side chains are indicated by "+" and "−" symbols. (A) Wild type, showing the salt bridge between Asp 308 and Lys 311.(B) Mutant E(D308K/K311E), showing a hypothetical salt bridge in reversed orientation. (C) Mutant E(T310K), with a Thr-to-Lys substitution at position 310. (D) Mutant E(T310K/K311E), showing a potential reorientation of the side chains at positions 310 and 308 due to an additional Lys-to-Glu substitution at position 311.

was apparently tolerated by the virus. It was reported previously that mutations at position 308 strongly impaired the neurovirulence of the closely related LI virus (3, 9). Our data only partially support this observation. In the adult mouse model, mutant E(D308E) was shown to have impaired infectivity but a wild-type attenuation index (LD_{50}/ID_{50} ratio). The double mutant E(D308H/K311E) was found to be attenuated for virulence but also impaired with respect to peripheral infectivity and cell culture growth parameters. Moreover, this mutant exhibited heterogeneous plaque morphologies (Table 2) and a peculiar nonlinear dose-response relationship at intermediate inoculation doses in the adult mouse model (not shown). In two independent experiments we observed lower survival and infection rates at a lower inoculation dose than at the next higher one (data not shown). At this time we cannot explain this phenomenon, which has not been observed for any of the other mutants investigated in this or previous studies.

The fact that only minor effects were observed after the mutagenesis of Lys 309 came as a surprise. This large and positively charged residue is conserved among all tick-borne flaviviruses but is lacking in mosquito-borne flaviviruses, suggesting an important functionality within the tick-borne group. Changing this residue into a nonpolar Leu had hardly any effect in our test systems. Deletion of Lys 309 at first seemed to be deleterious, but a spontaneously arising second-site mutation (Phe 332 to Tyr; Fig. 2) was apparently able to compensate structurally for this defect, resulting in a mutant virus with an almost wild-type phenotype. Inspection of mosquito-borne flavivirus sequences reveals that several of them also have a Tyr residue in the position corresponding to Phe 332 in TBE virus. From our experiments one can conclude that Lys 309 is not crucial for function in cell culture and mice.

Of the mutations described in this study, position 310 clearly represents the most promising starting point for the rational

design of novel attenuated flavivirus vaccines. However, our data also demonstrate some potential limitations of this approach: the achieved attenuation was accompanied by an unfavorable reduction of peripheral infectivity and the spontaneous appearance of a second-site mutation. This illustrates how easily the virus can compensate for a single point mutation and revert to a more virulent phenotype in an unpredictable manner. In comparison, the attenuation indices achieved by previously described mutants carrying deletions in the 3′-NCR were more than 10 times better than that observed for mutant E(T310K) in this study (16). Moreover, no phenotypic reversions were observed for the deletion mutants, and one may reason that mutations that are able to compensate for large deletions are less likely to emerge than second-site phenotypic suppression of single point mutations. Thus, the 3′-NCR deletions appear to be more promising in terms of both safety and maintaining sufficient peripheral infectivity. For optimal attenuation and vaccine safety it is reasonable to develop virus mutants that combine different attenuating principles. The two 3′-NCR deletion and Lys 310 combination mutants described in this study in fact turned out to be virtually apathogenic. However, the significant increase of the LD_{50} that was achieved by combining these mutations was accompanied by a severe reduction in peripheral infectivity. Both mutants also exhibited a restricted cell culture growth and, with regard to vaccine development, these mutants might already have to be considered "overattenuated," although the seroconversion induced by these mutants still conferred a solid protective immunity. To achieve stable and sufficient attenuation by simultaneously retaining good growth properties and a high peripheral infectivity, it will probably be necessary to test various combinations of attenuating mutations and carry out an elaborate "fine-tuning" of their biological effects. The mutants constructed and characterized in this study provide relevant information for this ongoing process. In addition, they may be helpful in the future for studying the interaction of TBE virus with the cell surface during viral entry.

ACKNOWLEDGMENTS

We gratefully acknowledge the excellent technical assistance of Heide Dippe, Jutta Ertl, Silvia Röhnke, and Melby Wilfinger.

REFERENCES

1. **Chambers, T. J., M. Halevy, A. Nestorowicz, C. M. Rice, and S. Lustig.** 1998. West Nile virus envelope proteins: nucleotide sequence analysis of strains differing in mouse neuroinvasiveness. J. Gen. Virol. **79:**2375–2380.
2. **Chen, Y., T. Maguire, R. E. Hileman, J. R. Fromm, J. D. Esko, R. J. Linhardt, and R. M. Marks.** 1997. Dengue virus infectivity depends on envelope protein binding to target cell heparan sulfate. Nat. Med. **3:**866–871.
3. **Gao, G. F., M. H. Hussain, H. W. Reid, and E. A. Gould.** 1994. Identification of naturally occuring monoclonal antibody escape variants of louping ill virus. J. Gen. Virol. **75:**609–614.
4. **Hahn, C. S., J. M. Dalrymple, J. H. Strauss, and C. M. Rice.** 1987. Comparison of the virulent Asibi strain of yellow fever virus with the 17D vaccine strain derived from it. Proc. Natl. Acad. Sci. USA **84:**2019–2023.
5. **Heinz, F. X., R. Berger, W. Tuma, and C. Kunz.** 1983. A topological and functional model of epitopes on the structural glycoprotein of tick-borne encephalitis virus defined by monoclonal antibodies. Virology **126:**525–537.
6. **Heinz, F. X., W. Tuma, F. Guirakhoo, and C. Kunz.** 1986. A model study of the use of monoclonal antibodies in capture enzyme immunoassays for antigen quantification exploiting the epitope map of tick-borne encephalitis virus. J. Biol. Stand. **14:**133–141.
7. **Holzmann, H., K. Stiasny, M. Ecker, C. Kunz, and F. X. Heinz.** 1997. Characterization of monoclonal antibody-escape mutants of tick-borne encephalitis virus with reduced neuroinvasiveness in mice. J. Gen. Virol. **78:** 31–37.
8. **Jennings, A. D., C. A. Gibson, B. R. Miller, J. H. Mathews, C. J. Mitchell, J. T. Roehrig, D. J. Wood, F. Taffs, B. K. Sil, S. N. Whitby, J. E. Whitby, T. P. Monath, P. D. Minor, P. G. Sanders, and A. D. T. Barrett.** 1994. Analysis of a yellow fever virus isolated from a fatal case of vaccine-associated human encephalitis. J. Infect. Dis. **169:**512–518.
9. **Jiang, W. R., A. Lowe, S. Higgs, H. Reid, and E. A. Gould.** 1993. Single amino acid codon changes detected in louping ill virus antibody-resistant mutants with reduced neurovirulence. J. Gen. Virol. **74:**931–935.
10. **Kimura, T., J. Kimura-Kuroda, K. Nagashima, and K. Yasui.** 1994. Analysis of virus-cell binding characteristics on the determination of Japanese encephalitis virus susceptibility. Arch. Virol. **139:**239–251.
11. **Kopecky, J., L. Grubhoffer, V. Kovar, L. Jindrak, and D. Vokurkova.** 1999. A putative host cell receptor for tick-borne encephalitis virus identified by anti-idiotypic antibodies and virus affinoblotting. Intervirology **42:**9–16.
12. **Kuhn, R. J., and M. G. Rossmann.** 1995. When it's better to lie low. Nature **375:**275–276.
13. **Lin, B., C. R. Parrish, J. M. Murray, and P. J. Wright.** 1994. Localization of a neutralizing epitope on the envelope protein of dengue virus type 2. Virology **202:**885–890.
14. **Lobigs, M., R. Usha, A. Nestorowicz, I. D. Marshall, R. C. Weit, and L. Dalgarno.** 1990. Host cell selection of Murray Valley encephalitis virus variants altered at an RGD sequence in the envelope protein and in mouse virulence. Virology **176:**587–595.
15. **Mandl, C. W., M. Ecker, H. Holzmann, C. Kunz, and F. X. Heinz.** 1997. Infectious cDNA clones of tick-borne encephalitis virus European subtype prototypic strain Neudoerfl and high virulence strain Hypr. J. Gen. Virol. **78:** 1049–1057.
16. **Mandl, C. W., H. Holzmann, T. Meixner, S. Rauscher, P. F. Stadler, S. L. Allison, and F. X. Heinz.** 1998. Spontaneous and engineered deletions in the 3′ noncoding region of tick-borne encephalitis virus: construction of highly attenuated mutants of a flavivirus. J. Virol. **72:**2132–2140.
17. **McMinn, P. C.** 1997. The molecular basis of virulence of the encephalitogenic flaviviruses. J. Gen. Virol. **78:**2711–2722.
18. **Monath, T. P., and F. X. Heinz.** 1996. Flaviviruses, p. 961–1034. *In* B. N. Fields, D. M. Knipe, P. M. Howley et al. (ed.), Fields virology, 3rd ed. Lippincott-Raven Publishers, Philadelphia, Pa.
19. **Munoz, M. D., A. Cisneros, J. Cruz, P. Das, R. Tovar, and A. Ortega.** 1998. Putative dengue virus receptors from mosquito cells. FEMS Microbiol. Lett. **168:**251–258.
20. **Rauscher, S., C. Flamm, C. W. Mandl, F. X. Heinz, and P. F. Stadler.** 1997. Secondary structure of the 3′-noncoding region of flavivirus genomes: comparative analysis of base pairing probabilities. RNA **3:**779–791.
21. **Reed, J. L., and H. Muench.** 1938. A simple method for estimating fifty percent endpoints. Am. J. Hyg. **27:**493.
22. **Rey, F. A., F. X. Heinz, C. Mandl, C. Kunz, and S. C. Harrison.** 1995. The envelope glycoprotein from tick-borne encephalitis virus at 2 Å resolution. Nature **375:**291–298.
23. **Rice, C. M.** 1996. *Flaviviridae*: the viruses and their replication, p. 931–960. *In* B. N. Fields, D. M. Knipe, P. M. Howley et al. (ed.), Fields virology, 3rd ed. Lippincott-Raven Publishers, Philadelphia, Pa.
24. **Ruggli, N., and C. M. Rice.** 1999. Functional cDNA clones of the *Flaviviridae*: strategies and applications. Adv. Virus Res. **53:**183–207.
25. **Ruoslathi, E.** 1997. RGD and other recognition sequences for integrins. Annu. Rev. Cell. Dev. Biol. **12:**697–715.
26. **Ryman, K. D., T. N. Ledger, G. A. Campbell, S. J. Watowich, and A. D. T. Barrett.** 1998. Mutation in a 17D-204 vaccine substrain-specific envelope protein epitope alters the pathogenesis of yellow fever virus in mice. Virology **244:**59–65.
27. **Salas-Benito, J. S., and R. M. Del Angel.** 1997. Identification of two surface proteins from C6/36 cells that bind dengue type 4 virus. J. Virol. **71:**7246–7252.
28. **van der Most, R. G., J. Corver, and J. H. Strauss.** 1999. Mutagenesis of the RGD motif in the yellow fever virus 17D envelope protein. Virology **265:** 83–95.
29. **Wallner, G., C. W. Mandl, C. Kunz, and F. X. Heinz.** 1995. The flavivirus 3′-noncoding region: extensive size heterogeneity independent of evolutionary relationships among strains of tick-borne encephalitis virus. Virology **213:**169–178.
30. **Wallner, G., C. W. Mandl, M. Ecker, H. Holzmann, S. Stiasny, C. Kunz, and F. X. Heinz.** 1996. Characterization and complete genome sequences of high- and low-virulence variants of tick-borne encephalitis virus. J. Gen. Virol. **77:** 1035–1042.
31. **Wengler, G., D. W. Bradley, M. S. Collett, F. X. Heinz, R. W. Schlesinger, and J. H. Strauss.** 1995. Flaviviridae, p. 415–427. *In* F. A. Murphy, C. M. Fauquet, D. H. L. Bishop, S. A. Ghabrial, A. W. Jarvis, G. P. Martelli, M. A. Mayo, and M. D. Summers (ed.), Virus taxonomy. Sixth report of the International Committee on Taxonomy of Viruses. Springer, Vienna, Austria.